Available online at www.sciencedirect.com

SciVerse ScienceDirect

Ceramics International 39 (2013) S601–S604

CERAMICS INTERNATIONAL

www.elsevier.com/locate/ceramint

Microstructure and performance of micro-tubular solid oxide fuel cells made by aqueous electrophoretic deposition

J.S. Cherng[a,*], C.C. Wu[a], W.H. Chen[a], T.H. Yeh[b]

[a]*Department of Materials Engineering, MingChi University of Technology, 84 Gungjuan Rd., Taishan, Taipei 243, Taiwan*
[b]*Center for Thin Film Technologies and Applications, MingChi University of Technology, 84 Gungjuan Rd., Taishan, Taipei 243, Taiwan*

Available online 17 October 2012

Abstract

Anode-supported micro-tubular solid oxide fuel cells (SOFCs) were manufactured by consecutive aqueous electrophoretic depositions (EPDs) of porous anode layer (8YSZ–NiO), dense electrolyte layer (8YSZ) and porous cathode layer (LSM) onto a thin Cu wire, followed by stripping, drying, and a single-step co-sintering. The microstructure of the micro-tubular SOFC, including the thickness and porosity of each layer, was controlled by the processing parameters such as solid loading, current density, surfactant concentration and sintering temperature. The electrochemical performance of such a micro-tubular SOFC was demonstrated by the V–I–P (voltage–current–power) and impedance measurements.

Keywords: Electrophoretic deposition; Micro-tubular SOFC; Yttria-stabilized zirconia

1. Introduction

Micro-tubular solid oxide fuel cell (SOFC) [1–6] has emerged as a new class of SOFC design, which in principle can benefit from both the intrinsically higher efficiency of planar design and the easier packaging of tubular design, owing to its increase of the reactive area per unit volume. However, most researchers in this field employed such manufacturing methods as extrusion and dip coating which might suffer from their poor controllability and repeatability, etc.

In our previous study [7] we have demonstrated a novel method to make micro-tubular SOFC which utilizes aqueous electrophoretic deposition (EPD) to consecutively deposit the anode, electrolyte, and cathode layers on a thin Cu wire, followed by stripping, drying and a single-step co-sintering. Nevertheless, it was 3YSZ (3 mol% yttria-stabilized zirconia) instead of 8YSZ (8 mol% yttria-stabilized zirconia) that was chosen in that demonstration since the former is cheaper and more familiar to us to handle. Therefore, a far-from-satisfactory cell performance, 3.5 mW/cm^2, at 800 °C was recorded during that study. In the present paper, 8YSZ is employed as the electrolyte and the ceramic component of the 8YSZ–Ni cermet anode as well. Both the microstructural developments and electrochemical properties of such a more realistic micro-tubular SOFC will be addressed accordingly.

2. Experimental

NiO (NiO–F, Inco) and 8YSZ (HSY-8.0, Daiichi Kigenso) powders, according to a 7:3 ratio, were mixed and attrition milled in distilled water. Suspensions with various solid loading of such anode (8YSZ–Ni cermet, upon reduction at work), electrolyte (8YSZ) and cathode ($La_{0.8}Sr_{0.2}MnO_3$, LSM, Ningbo Institute of Material Technology and Engineering) ceramic powders, respectively, were made by mixing the powders with distilled water using a shear mixer and an ultrasonic sonicator. To prevent the colloids from agglomeration and sedimentation, suitable amount of ammonium polyacrylate (PAA-NH_4, Darvan821A, R.T. Vanderbilt, USA) was added as dispersant. PAA-NH_4 would dissociate in water so that PAA- ions would adsorb to ceramic particles to stabilize them electrosterically. Zeta potentials of these suspensions were determined by laser Doppler velocimetry. The details of suspension preparation and evaluation, as

*Corresponding author. Tel.: +886 2 29089899; fax: +886 2 29084091.
E-mail address: cherng@mail.mcut.edu.tw (J.S. Cherng).

0272-8842/$ - see front matter © 2012 Elsevier Ltd and Techna Group S.r.l. All rights reserved.
http://dx.doi.org/10.1016/j.ceramint.2012.10.144

well as the setup of constant-current EPD can be found elsewhere [8].

The EPD cell consisted of a Cu wire (150 μm φ) anode surrounded by a hollow cylinder Ni cathode in one of the aforementioned suspensions. The distance between these two electrodes was 1.5 cm. EPD was conducted under constant current control at various current levels. The process of a micro-tubular SOFC was carried out by EPD (8YSZ–NiO)→drying→EPD (8YSZ)→drying→EPD (LSM), then followed by stripping from the Cu wire, complete drying, and co-sintering at 1250 °C for 2 h in order to obtain a final structure consisting of a porousanode layer, a dense electrolyte layer and a porous cathode layer respectively. The microstructure was revealed by SEM, and the porosity was stereometrically measured by a linear intercept method. The electrochemical performance of the micro-tubular SOFC was investigated by impedance analysis and the V–I–P (voltage–current–power) measurements.

3. Results and discussion

Fig. 1(a) shows the variations of zeta potential with pH value for slurries of 8YSZ, NiO, 8YSZ–NiO, and 3YSZ–NiO (as a comparison) respectively. It is observed that the suspension behavior of the 8YSZ–NiO mixture is controlled by NiO up to pH 8, then jointly influenced by both the components at higher pH values. This is different from that of 3YSZ–NiO where NiO dominates throughout the complete pH range. However, the scenario changed by the very similar variations of zeta potential with PAA-NH_4 addition for both NiO and 8YSZ–NiO mixture, as shown in Fig. 1(b). Note that the zeta potential of 8YSZ–NiO levels at a less negative value than that of 3YSZ–NiO by about 10 mV, indicating a worse suspension obtained than the latter. Although only the electrostatic part of, rather than the whole electrosteric, stabilization is measured by zeta potential, the data in Fig. 1(b) nevertheless suggests that about 0.6 wt% of PAA-NH_4 is required for a good suspension of the 8YSZ–NiO mixture. Similar results can be obtained for the suspension behaviors of 8YSZ and LSM as well.

The addition of PAA-NH_4 not only improves the suspension of the slurry, but also affects the packing density (thus the sintered density too) and deposition rate during EPD. An example is given in Fig. 2 which plots the effects of PAA-NH_4 addition on the 1250 °C-sintered density of single-layered LSM, 8YSZ, and 8YSZ–NiO respectively. It is observed that in the over-saturated adsorption regime (e.g., >0.6 wt% of PAA-NH_4 for 8YSZ–NiO), the porosity of sintered ceramics increases with PAA-NH_4 concentration. This could be due to the freely suspended and EPD-deposited PAA^- left within the deposit and then contributes to the porosity during sintering. The effects of other major processing parameters during EPD like solid loading and applied current could also be similarly investigated as in our previous study [7].

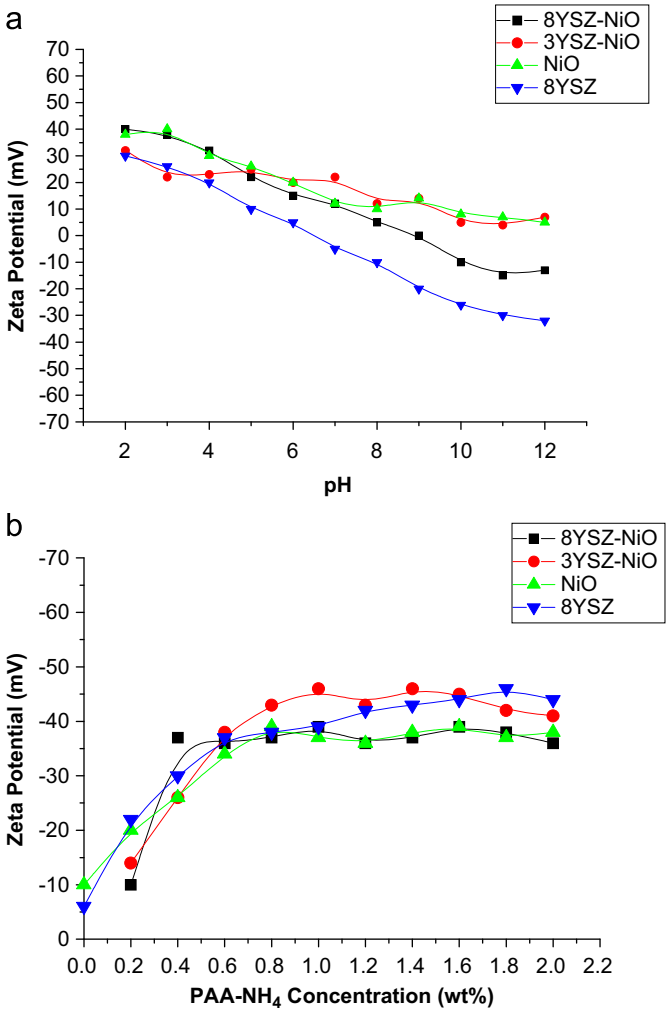

Fig. 1. Variations of zeta potential with: (a) pH, and (b) PAA-NH_4 concentration for YSZ, NiO and their mixtures.

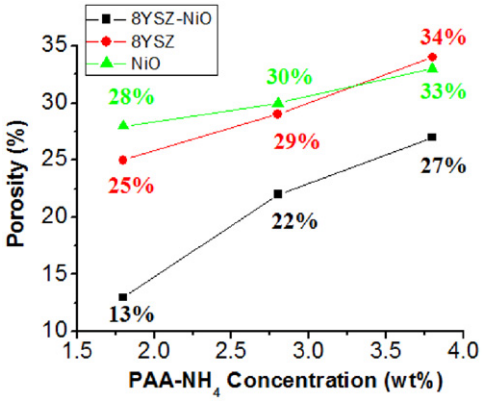

Fig. 2. Effects of PAA-NH_4 addition on the 1250 °C-sintered density of single-layered LSM, 8YSZ, and 8YSZ–NiO respectively. EPD at a solid loading of 10 wt% and 5 mA.

Although 1250 °C seems not enough to fully densify a single 8YSZ layer, a one-step co-sintering at the same temperature nevertheless is sufficient to produce a micro-tubular SOFC with porous 8YSZ–NiO anode/dense 8YSZ

electrolyte/porous LSM cathode 3-layeredstructure as demonstrated in Fig. 3. It thus appears that the differential sintering stresses built up in between the anode/electrolyte/cathode interfaces actually helps to densify the thin 8YSZ electrolyte layer. The detailed EPD conditions for this sample are shown in Table 1.

The electrochemical performance of such a micro-tubular SOFC can be seen in Fig. 4 where the V–I–P analysis is carried out at 600–800 °C with a 50 sccm fuel of 20% H_2 in N_2 flowing inside the tube and air outside. The about 1 V open circuit voltage (V_{oc}), near the theoretical value estimated from the Nernst equation, verified the gas-tightness of the 8YSZ electrolyte layer. The optimum power density at 800 °C reaches 363.8 mW/cm^2 which is comparable to the literature records, not to mention that there are clearly much more room to improve further, say, by using thinner 8YSZ electrolyte layer and purer fuel gas, as well as by optimizing the porosities/thicknesses of the anode/cathode layers, etc.

Fig. 5 shows the AC-impedance (42 Hz–1 MHz) spectra, measured at 500–800 °C, of such a micro-tubular SOFC as shown in Fig. 4. The left intercepts of the arcs with the real axis are taken as the resistances (R) of the electrolyte (from grain interior and grain boundary) at various temperatures. Knowing the thickness (L) and area (A) in contact with the cathode, we computed the conductivity

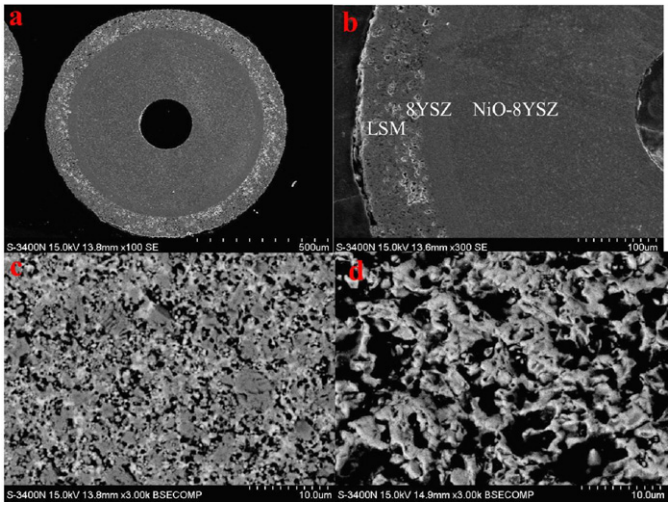

Fig. 3. (a) A typical scanning electron micrograph of a micro-tubular SOFC (one-step co-sintered at 1250 °C) electrophoretically deposited at conditions shown in Table 1. (b)–(d) Close-ups showing a dense YSZ electrolyte layer about35 μm, a cermet anode layer with 32% porosity, and a cathode LSM layer with 42% porosity.

Table 1
The EPD conditions of the sample in Fig. 3.

Slurry	8YSZ–NiO	8YSZ	LSM
Solid loading (wt%)	10	30	10
Current (mA)	2	10	5
PAA-NH_4 (wt%)	3.8	1.8	2.0

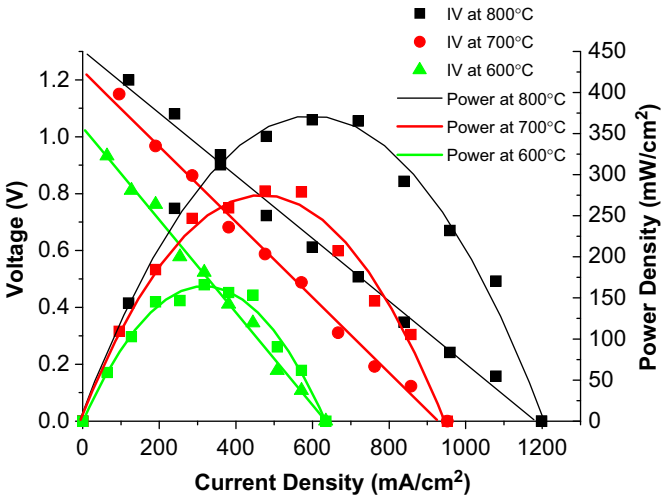

Fig. 4. Electrochemical performance of such a micro-tubular SOFC as shown in Fig. 3. The V–I–P analysis is carried out with a 50 sccm fuel of 20% H_2 in N_2 flowing inside the tube and air outside.

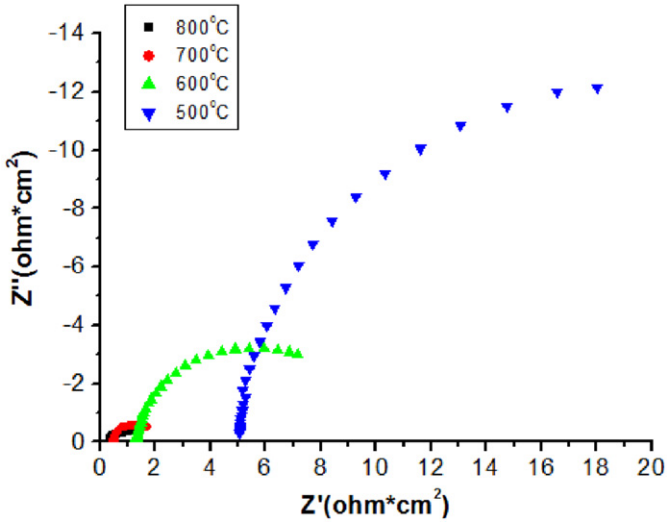

Fig. 5. Impedance spectra of such a micro-tubular SOFC as shown in Fig. 4, measured at 500–800 °C.

(σ) according to

$$\sigma = L/(AR) \quad (1)$$

The conductivity of 8YSZ as a function of temperature typically follows Arrhenius-type behavior

$$\sigma = \sigma_o \exp\left(-E_a/kT\right) \quad (2)$$

where k is the Boltzman constant, σ_o the pre-exponential constant, and E_a the activation energy for conduction. Shown in Fig. 6 is an Arrhenius plot of the logarithm of electrolyte conductivity as a function of 1/T, with the data taken from Fig. 5. Also shown in Fig. 6 is the data of bulk 8YSZ [9] as a comparison. It shows that our EPD 8YSZ has a lower activation energy, 67.4 kJ/mole, than that of the reference 8YSZ, 89.6 kJ/mole. This difference could be attributed to the different chemical compositions of the

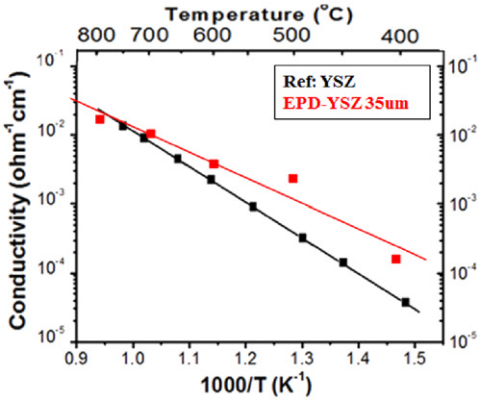

Fig. 6. Arrhenius plot of the logarithm of electrolyte conductivity as a function of 1/T, data taken from Fig. 5.

starting powders, as well as the lower sintering temperature used in our EPD-deposited sample. There have been reports from the literature about the effects of sintering temperature on the ionic conductivity of YSZ [10–13]. Some of our preliminary analyses have even shown that higher sintering temperature causes possible evaporation of yttrium thus reducing the concentration of oxygen vacancy and ionic conductivity. Further investigation is required to clarify this point.

Conclusions

Consecutive aqueous EPD plus single-step co-sintering have been successfully employed to make micro-tubular SOFC using 8YSZ as the ionic conductor. The resultant power density of a typical SOFC reaches 363.8 mW/cm^2 at 800 °C, with a relatively lower activation energy of 67.4 kJ/mole for ionic conduction of our EPD-deposited and low-temperature-sintered 8YSZ.

Acknowledgment

The financial support by The National Science Council of Taiwan (NSC100-2221-E-131-015) is appreciated.

References

[1] N.M. Sammes, Y. Du, R. Bove, Design and fabrication of a 100 W anode supported micro-tubular SOFC stack, Journal of Power Sources 145 (2005) 428–434.
[2] S.B. Lee, T.H. Lim, R.H. Song, D.R. Shin, S.K. Dong, Development of a 700 W anode-supported micro-tubular SOFC stack for APU applications, International Journal of Hydrogen Energy 33 (2008) 2330–2336.
[3] T. Suzuki, T. Yamaguchi, Y. Fujishiro, M. Awano, Fabrication and characterization of micro tubular SOFCs for operation in the intermediate temperature, Journal of Power Sources 160 (2006) 73–77.
[4] T. Suzuki, Y. Funahashi, T. Yamaguchi, Y. Fujishiro, M. Awano, Anode-supported micro tubular SOFCs for advanced ceramic reactor system, Journal of Power Sources 171 (2007) 92–95.
[5] T. Suzuki, T. Yamaguchi, Y. Fujishiro, M. Awano, Current collecting efficiency of micro tubular SOFCs, Journal of Power Sources 163 (2007) 737–742.
[6] T. Suzuki, Y. Fujishiro, T. Yamaguchi, Y. Fujishiro, M. Awano, Fabrication and characterization of micro tubular SOFCs for advanced ceramic reactors, Journal of Alloys and Compounds 451 (2008) 632–635.
[7] J.S. Cherng, M.Y. Ho, T.H. Yeh, W.H. Chen, Anode-supported micro-tubular SOFCs made by aqueous electrophoretic deposition, Ceramics International 38S (2012) S477–S480.
[8] J.S. Cherng, J.R. Sau, C.C. Chung, Aqueous electrophoretic deposition of YSZ electrolyte layers for solid oxide fuel cells, Journal of Solid State Electrochemistry 12 (2007) 925–933.
[9] L. Yang, S. Wang, K. Blinn, M. Liu, Z. Liu, Z. Cheng, M. Liu, Enhanced sulfur and coking tolerance of a mixed ion conductor for SOFCs: $BaZr_{0.1}Ce_{0.7}Y_{0.2-x}Yb_xO_{3-d}$, Science 326 (2009) 126–129.
[10] X.J. Chen, K.A. Khor, S.H. Chan, L.G. Yu, Influence of microstructure on the ionic conductivity of yttria-stabilized zirconia electrolyte, Materials Science and Engineering A A355 (2002) 246–252.
[11] T. He, Z. Lu, L. Pei, X. Huang, Z. Liu, W. Su, Electrical Properties of thin-walled 8 mol% yttria-stabilized zirconia electrolyte tubes prepared by an improved slip casting method, Journal of Alloys and Compounds 333 (2002) 231–236.
[12] Z. Wang, K. Sun, S. Shen, X. Zhou, J. Qiao, N. Zhang, Effect of co-sintering temperature on the performance of SOFC with YSZ electrolyte thin films fabricated by dip-coating method, Journal of Solid State Electrochemistry 14 (2010) 637–642.
[13] T. Talebi, M. Haji, B. Raissi, Effect of sintering temperature on the microstructure, roughness and electrochemical impedance of electrophoretically deposited YSZ electrolyte for SOFCs, International Journal of Hydrogen Energy 35 (2010) 9420–9426.